

# Performance study of a micro-pattern gas detector: leak microstructure<sup>\*</sup>

ZHANG Ai-Wu(章爱武)<sup>1,2;1)</sup> XIE Yu-Guang(谢宇广)<sup>1</sup> YU Bo-Xiang(俞伯祥)<sup>1</sup>  
 AN Zheng-Hua(安正华)<sup>1</sup> WANG Zhi-Gang(王志刚)<sup>1</sup> CAI Xiao(蔡啸)<sup>1</sup> SUN Xi-Lei(孙希磊)<sup>1</sup>  
 SHI Feng(石峰)<sup>1</sup> FANG Jian(方建)<sup>1</sup> XUE Zhen(薛镇)<sup>1</sup> LÜ Qi-Wen(吕绮雯)<sup>1,4</sup>  
 SUN Li-Jun(孙丽君)<sup>1</sup> GE Yong-Shuai(葛永帅)<sup>1</sup> LIU Ying-Biao(刘颖彪)<sup>1</sup>  
 LIU Hong-Bang(刘宏邦)<sup>2,3</sup> ZHENG Yang-Heng(郑阳恒)<sup>2</sup> XIE Yi-Gang(谢一冈)<sup>2</sup>  
 HU Tao(胡涛)<sup>1</sup> ZHOU Li(周莉)<sup>1</sup> LÜ Jun-Guang(吕军光)<sup>1</sup>

<sup>1</sup> State Key Laboratory of Particle Detection and Electronics, Institute of High Energy Physics,  
 Chinese Academy of Sciences, Beijing 100049, China

<sup>2</sup> Graduate University of Chinese Academy of Sciences, Beijing 100049, China

<sup>3</sup> Guangxi University, Nanning 530004, China

<sup>4</sup> Shanxi University, Taiyuan 030006, China

**Abstract:** A micro-pattern gas detector named leak microstructure (LM) has been studied. A new chemical electrolytic technique is introduced to make perfect shaped LM needles with very sharp tips, and this method may be developed to make LM array detectors in batches. The experimental results are presented for both a single needle LM detector and a small LM array detector. The gas gain is up to  $10^5$  by calculation from the waveform. Good gain stability and uniformity are achieved. The light emission from the needle tip is also measured in Ar/CF<sub>4</sub>(95/5) gas mixture. The result shows a promising application for imaging.

**Key words:** leak microstructure (LM), electrolytic technique, gas gain, light emission

**PACS:** 29.40.Cs, 29.40-n, 07.85.Fv **DOI:** 10.1088/1674-1137/36/10/012

## 1 Introduction

The micro-pattern gas detectors (MPGD) have experienced a flourishing development in past decades. Many kinds of micro-structure detectors have been put forward and investigated, among which the hole structures (like GEM, THICK GEM) [1–3] and micro mesh structure (MICROMEAS) [4] achieved great success. The concept of micro-point (or pin) geometry came forth in the 1980s [5–7]. A typical example is the leak microstructure (LM) detector, which has been proposed since 1997 [8]. The LM detector has good energy resolution of 8% (FWHM) and fast signal response of 20–30 ns width working in the proportional region, and its gas gain is up to  $6.6 \times 10^5$  in iso-butane and about one order of magnitude less

in Ar/methane (90/10) [9]. The potential of the LMs in X-ray imaging [10], single-electron counting [11] and other applications [12] has been reported. The measurement of electron avalanches in liquid argon mixtures with LM has also been studied [13].

In this work, a new chemical electrolytic technique is introduced to produce suitable LM needles. Compared with the traditional craft, this method is relatively cheap and might be easier to make needle arrays in the laboratory. The electric field distribution and the electron avalanche in the LM detector are simulated by MAXWELL [14] and GARFIELD [15], respectively. The experimental results are presented, including the gas gain, operation modes, spectrum characteristics and so on. The possibility of its applications in high energy physics is also discussed.

Received 2 February 2012

<sup>\*</sup> Supported by National Natural Science Foundation of China (10775151), Youth Fund of Institute of High Energy Physics, Chinese Academy of Sciences, Foundation of the State Key Laboratory of Particle Detection and Electronics of IHEP

1) E-mail: zhangaw@ihep.ac.cn

©2012 Chinese Physical Society and the Institute of High Energy Physics of the Chinese Academy of Sciences and the Institute of Modern Physics of the Chinese Academy of Sciences and IOP Publishing Ltd

## 2 Configuration of the LM detector

The LM detector consists of tungsten-needles (with tip less than  $30\ \mu\text{m}$ ) or gold-plated tungsten wires (diameter no more than  $100\ \mu\text{m}$  and without tip) acting as anode, a copper coated PCB plate with insulating holes (diameter  $300\ \mu\text{m}$ ) as cathode, and a drift electrode several millimeters above the cathode. The needles are required to be well centered in the circular holes, perpendicular to the cathode plane, and the needle tips are  $100\text{--}500\ \mu\text{m}$  higher than the cathode plane as shown in Fig. 1.

The principle of an LM detector is described as follows. An avalanche will take place around the tip of the needle due to the local, strong electric field. The avalanched electrons will drift to the tip and the ions will drift to the cathode, which produce very fast negative signals on the anode.

In principle, the gold-plated tungsten wires can be used. However, it is difficult to handle them in the laboratory. Thus the tungsten-needles are more suitable for the anodes in this work.

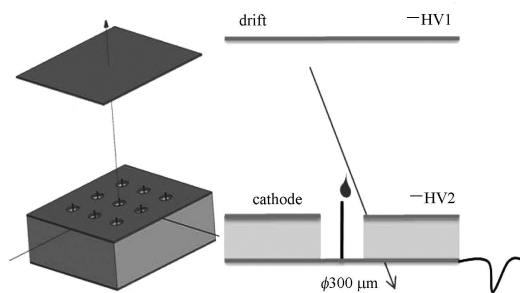
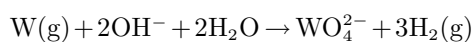


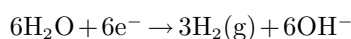
Fig. 1. The configuration and principle of the LM detector. The diameter of the hole and the tip of needle are  $300\ \mu\text{m}$  and  $40\ \mu\text{m}$  respectively.

As the first step, a special needle with tip around  $30\ \mu\text{m}$  was produced by an electrochemical method. The electrolysis setup is shown in Fig. 2(a). The electrolyte is  $2\ \text{mol/L NaOH}$  solution, and the electrochemical reaction equations are shown as follows [16]:

Anodic,



Cathodic,



In the electrolysis procedure, a  $\phi 300\ \mu\text{m}$  tungsten wire is put several millimeters perpendicularly

into the center of an annular stainless steel cathode, which is immersed in the electrolyte. A DC power is connected to the wire and normally  $18\ \text{V}$  is applied to start the reaction. The electric current varies from  $3\ \text{A}$  to  $0\ \text{A}$ , and finally the tungsten wire is divided into two parts from the liquid level by gravity action. The remaining tungsten wire above the liquid level has a suitable tip and can be clipped as an LM needle. About 300 needles were produced with this method, and  $\frac{2}{3}$  of them were with good consistence, the mean length-diameter ratio of the needle and its deviation was 2.74 and 0.09 respectively, and the tip of the needles was about  $30\ \mu\text{m}$ . Fig. 2(b) shows one of the needles with  $30\ \mu\text{m}$  tip; it can be seen that the tip is similar to those used in literature [8]. Our experimental results are all based on these homemade needles.

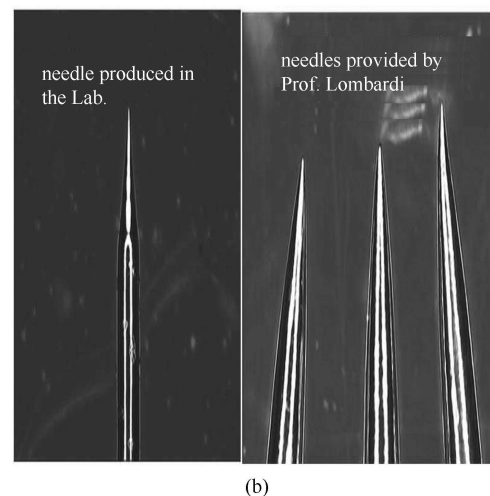
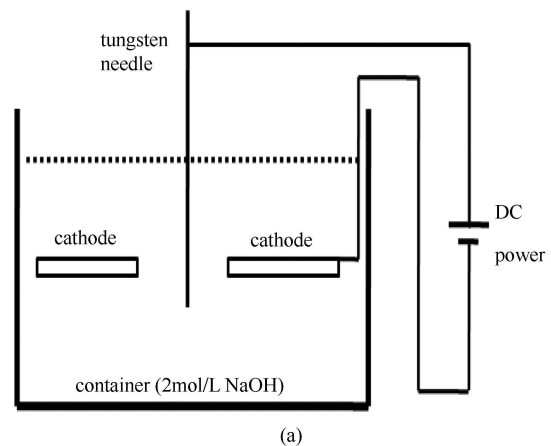
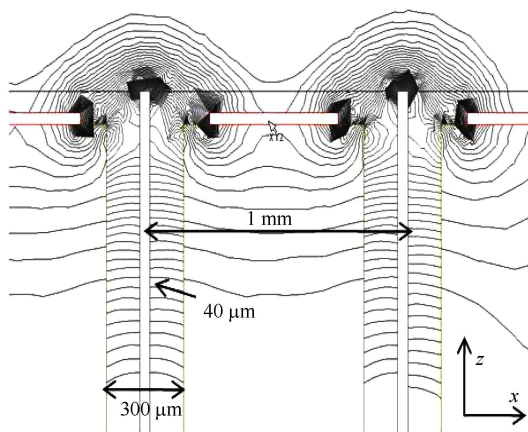


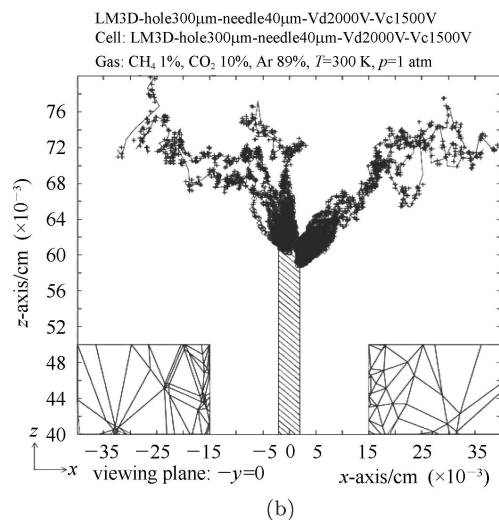
Fig. 2. (a) The electrolysis setup for producing the needles; (b) The tungsten needle produced in Lab (left) comparison with the needles used in literature (right, provided by Prof. Lombardi, INFN). The needle diameter is  $300\ \mu\text{m}$  and the tip is  $30\text{--}40\ \mu\text{m}$ .

### 3 Simulation of the LM detector

In order to better understand the LM detector's principle and optimize its geometry parameters, the electric field distribution and electron avalanche were simulated by MAXWELL [14] and GARFIELD [15] respectively. In the simulation, the hole size is  $300\ \mu\text{m}$ , the needle is  $40\ \mu\text{m}$ , the height is  $100\ \mu\text{m}$ , and the high voltage on the cathode is set to be  $-1500\ \text{V}$ . In this configuration, the electric field on the tip of the needle is close to the actual situation (where the needle appears to be cone-shaped). From Fig. 3(a) it can be seen that the strongest electric field is near the needle tips, and it can be up to  $10^7\ \text{V/m}$  with high voltage bias of  $-1500\ \text{V}$ . For the electron avalanche simulation,



(a)



(b)

Fig. 3. Simulation results of the LM detector. (a) Electric field distribution by MAXWELL and (b) Electron avalanche by GARFIELD (The hole size is  $300\ \mu\text{m}$ , the needle is  $40\ \mu\text{m}$  and the height is  $100\ \mu\text{m}$ . The high voltage on the cathode is  $-1500\ \text{V}$ ).

electrons are randomly produced in  $0.2\ \text{mm}$  above the cathode plane. Fig. 3(b) shows that the avalanches mainly happen within a  $100\ \mu\text{m}$  sphere around the needle tip, and create the clear ionization tracks.

### 4 Experimental setup

The LM detector used for our studies is illustrated in Fig. 4. Fig. 4(a) shows a test chamber made of methyl methacrylate, in which the drift region is  $3\ \text{mm}$  above the cathode plane. Fig. 4(b) is an enlarged photograph of a single needle LM. Fig. 4(c) shows a  $5\times 5$  array and Fig. 4(d) is the side-view of the LM, where the height of the needle is  $0.2\ \text{mm}$ .

The signals can be read out by either an oscilloscope directly or with amplifiers. For the former, a Tektronix TDS 3000 oscilloscope was used to measure the ultimate gas gain of the LM detector. For the latter, an Ortec 142AH charge sensitive preamplifier and an Ortec 450 primary amplifier are combined and followed by an Ortec TRUMP PCI 8 K multi channel analyzer (MCA). The operation modes, energy response, stability and uniformity of the LM detector were studied with these electronic readout systems.

Two types of gas mixtures were used for the experiment:  $\text{Ar}/\text{CO}_2/\text{CH}_4(89/10/1)$  and  $\text{Ar}/\text{CF}_4(95/5)$ . All the tests were done at atmospheric pressure.

### 5 Results of the single LM

#### 5.1 Operation modes

By investigating the signals without amplifiers, two kinds of operation modes were seen by using  $5.9\ \text{keV}\ ^{55}\text{Fe}$  X-ray. In  $\text{Ar}/\text{CO}_2/\text{CH}_4(89/10/1)$ , the pulse is very fast ( $40\ \text{ns}$  width), and the amplitude increases with the voltage. The maximum amplitude can reach  $25\ \text{mV}$ . In  $\text{Ar}/\text{CF}_4(95/5)$ , the signal becomes more complicated. The LM detector starts working at a lower voltage with fast signals; and when the voltage exceeds a critical value, its pulse suddenly becomes much wider ( $200\text{--}400\ \text{ns}$ ), while the amplitude ( $\sim 10\ \text{mV}$ ) only changes slightly (seems saturated and unrelated with energy). The typical pulses in these two gas mixtures are shown in Fig. 5(a). These results imply that the LM detector may work in the proportional mode in some gases with large quenching components such as  $\text{CO}_2$ , as well as the streamer mode in gases with luminescent elements like  $\text{CF}_4$ .

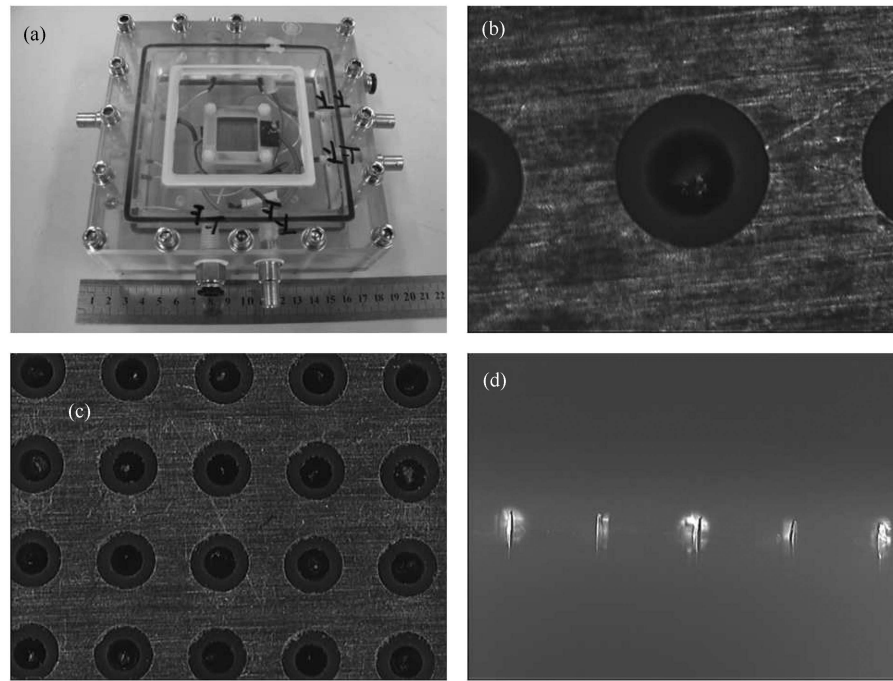


Fig. 4. The detector setup. (a) The detector chamber; (b) Single LM; (c) An LM array with 5 by 5 needles, the interval is 1 mm between each needle; (d) The side-view of the LM array. The black lines are the needles with 0.2 mm height above the cathode plane.

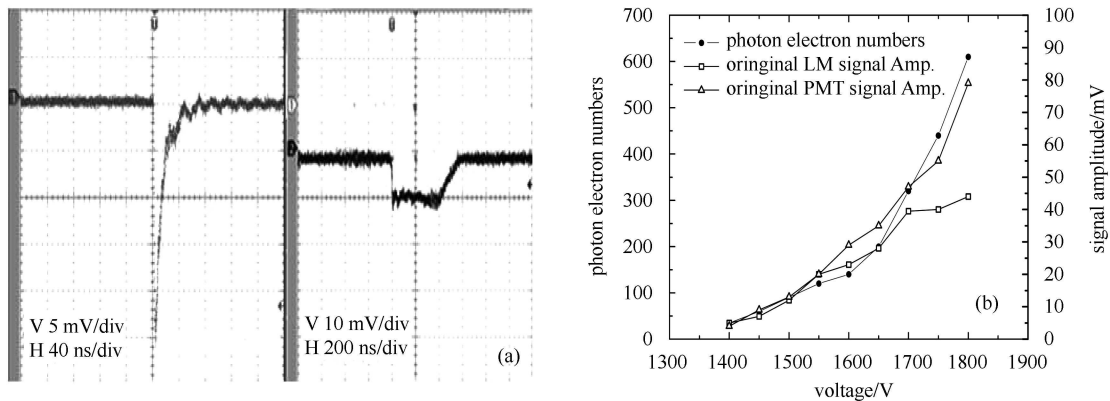


Fig. 5. The signal and light emission results of the LM detector with single needle. (a) The signals in different modes. The left (with 25 mV in amplitude and 40 ns in width) is in Ar/CO<sub>2</sub>/CH<sub>4</sub> (89/10/1) and the right (with 10 mV in amplitude and 400 ns in width) is in Ar/CF<sub>4</sub> (95/5); (b) The light emission of single LM measured by a PMT in Ar/CF<sub>4</sub> (95/5) for a single LM detector.

In the proportional mode, the gas gain is calculated to be  $4.5 \times 10^5$  from the waveform with formula  $G = VT/2ReN$ , where  $V$  is the amplitude ( $\sim 20$  mV),  $T$  is the signal width ( $\sim 40$  ns),  $R$  is  $50 \Omega$ ,  $e$  is the electron charge and  $N \sim 110$  is half of the primary ionization number. In the streamer mode, the quantity of the electric charge is 80 pC estimated by the area of the waveform, which is approximately  $\sim 10$  times larger than the charge of the proportional mode.

## 5.2 Light emission

The light emission of a single LM needle was measured by using a photomultiplier (XP2020) and a  $\gamma$  source ( $^{241}\text{Am}$ ). The photoelectron number ( $n_{pe}$ ) was calibrated by single photoelectron spectrum of the PMT. The result is shown in Fig. 5(b). It can be seen that the LM detector can work in the streamer mode in Ar/CF<sub>4</sub> (95/5) with very strong visible light emission.

The light emission intensity is proportional to the bias voltage applied, and  $n_{pe}$  is about 100~600 near the tip of the LM needle. The total photon numbers could be several times larger if considering the solid angle of the needle tip and the quantum efficiency of the PMT. Thus, this effect is very promising to be applied for X-ray imaging with CCDs.

### 5.3 Energy response

The energy spectra of different radiation sources were measured with the amplifier and MCA system. Only in Ar/CF<sub>4</sub> (95/5), the peaks in the spectra are observed. The 5.9 keV X-ray of <sup>55</sup>Fe is usually used

for measuring the energy resolution of a gas detector. However, for the LM detector, the escape peak of the <sup>55</sup>Fe source can hardly be detected due to incomplete collection of the primary electrons on the sharp needle tip and the non-uniform electric field around the tip that causes small differences in gain. In addition, much higher energies of  $\gamma$  rays (<sup>241</sup>Am, <sup>60</sup>Co) and  $\beta$  rays (<sup>90</sup>Sr) were also used. The shift of the peak positions is not significant as shown in Fig. 6. Therefore the signals of the LM detector may be saturated in Ar/CF<sub>4</sub> (95/5). Comparatively, the non-uniform electric field around the tip might result in the peak being undetectable in Ar/CO<sub>2</sub>/CH<sub>4</sub> (89/10/1).

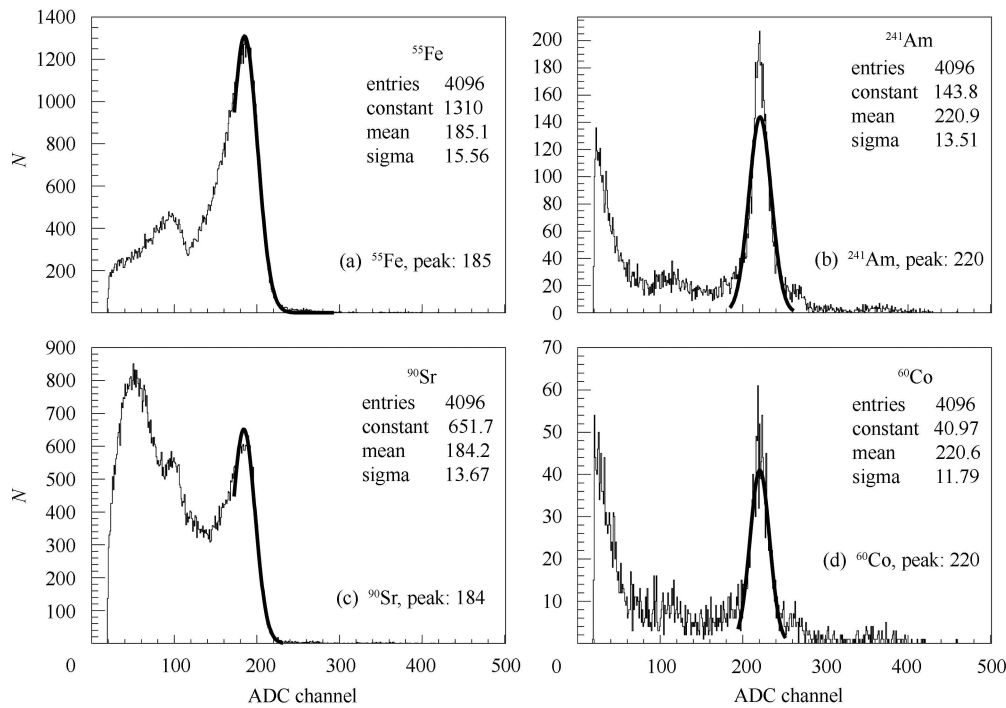


Fig. 6. The energy spectrum of different radiation sources in Ar/CF<sub>4</sub> (95/5).

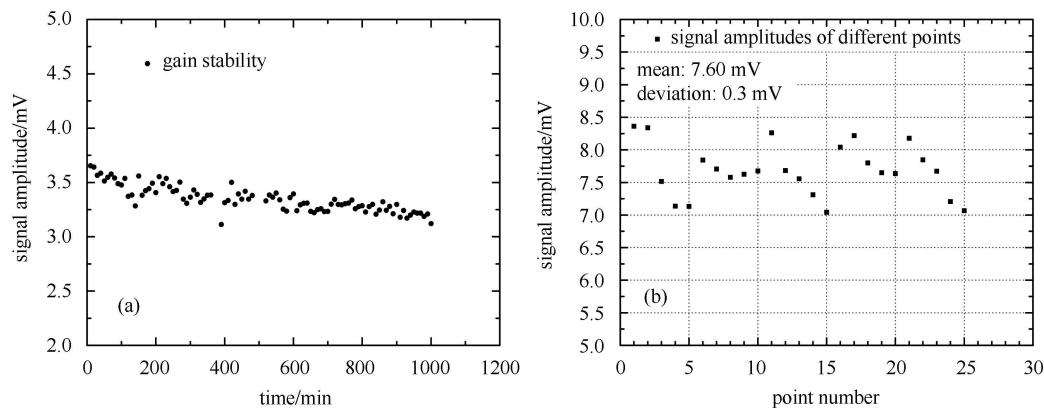


Fig. 7. (a) The gain stability of the LM array detector; (b) The signal amplitudes of different points.

## 6 Results of the LM array

It is obvious that the electric field is very sensitive to the needle shape. So, when an array of LM needles is made, it is critical to ensure that the needles have almost the same shape on the tips, as well as nearly identical protruding height from the cathode plane. At present, a  $5 \times 5$  LM array detector was made by hand (Fig. 4(c)), the needles were placed at 1 mm interval, and the height was 0.2 mm (Fig. 4(d)). The 25 needles were connected together as one channel for readout.

The gain stability was measured in Ar/CO<sub>2</sub>/CH<sub>4</sub> (89/10/1). Direct readout was chosen to monitor the gain stability, as shown in Fig. 7(a). The gain decreases faster in the first two hours and then tends to stabilise slowly.

Also, the gain uniformity was studied by measuring 25 points (with 1 mm pitch) over the needle array. As there was only one readout channel, a <sup>55</sup>Fe source was collimated above each needle and the signal amplitudes were measured by an oscilloscope. The measured amplitudes can be seen in Fig. 7(b). The mean amplitude and deviation are 7.60 mV and 0.30 mV respectively.

## 7 Discussion and conclusions

The study of the LM detector is still preliminary up to now. The chemical electrolytic technique is well suited to produce nice needles. The LM detector can work in the proportional and the streamer modes. The gas gain up to  $4 \times 10^5$  is reached, and the gain stability is achieved. The gain uniformity is very sensitive to the geometry alignment of the LM needles in an array.

Despite some shortcomings, the LM is still a promising micro-pattern gas detector. The higher gas gain is significant to reduce the cost of the front-end electronics. In addition, the strong light emission shows the potential for X-ray imaging with CCDs. The capability of the counting rate is estimated to be 10<sup>7</sup>Hz or higher because of the fast signals (less than 100 ns) and it is also possible for the LM to obtain prospective applications in some special regions, such as the liquid argon or xenon TPC detectors, where the serried needle array is not necessary.

*We would like to express our appreciation to Prof. M. Lombardi for his friendly discussions and supplying the needles.*

## References

- 1 Sauli F. Nucl. Instrum. Methods A, 1997, **386**: 531–534
- 2 Chechik R, Breskin A et al. Nucl. Instrum. Methods A, 2004, **535**: 303–308
- 3 Sarvestani A et al. Nucl. Instrum. Methods A, 1998, **410**: 238–258
- 4 Giomataris Y et al. Nucl. Instrum. Methods A, 1996, **376**: 29–35
- 5 Comby G et al. Nucl. Instrum. Methods, 1980, **174**: 77–92 (in French)
- 6 Comby G, Mangeot P. IEEE Trans. on Nucl. Sci., 1980, **NS-27**: 106–110
- 7 Bateman J E. Nucl. Instrum. Methods A, 1985, **238**: 524–532
- 8 Lombardi M, Lombardi F S. Nucl. Instrum. Methods A, 1997, **388**: 186–192
- 9 Lombardi M et al. Nucl. Instrum. Methods A, 2001, **461**: 91–95
- 10 Baiocchi C et al. Nucl. Instrum. Methods A, 2004, **518**: 448–451
- 11 Ferretti A et al. Nucl. Instrum. Methods A, 2009, **599**: 215–220
- 12 Nardo L De et al. Nucl. Instrum. Methods A, 2006, **562**: 127–135
- 13 Kim J G et al. Nucl. Instrum. Methods A, 2004, **534**: 376–396
- 14 Maxwell 2D\3D, Ansoft Co. Pittsburg PA, USA
- 15 Garfield. <http://garfield.web.cern.ch/garfield/>
- 16 WANG Ming-Huan et al. Journal of Transducer Technology, 2005, **24**(3): 24–26 (in Chinese)